Anuria, Omphalocele, and Perinatal Lethality in Mice Lacking the CD34-related Protein Podocalyxin

Regis Doyonnas,[1] David B. Kershaw,[2] Christian Duhme,[1] Helen Merkens,[1] Shierley Chelliah,[1] Thomas Graf,[3] and Kelly M. McNagny[1]

[1]*The Biomedical Research Centre, University of British Columbia, Vancouver, BC, Canada*
[2]*University of Michigan Medical Center, Department of Pediatrics, Ann Arbor, MI 48109*
[3]*Albert Einstein College of Medicine, Bronx, NY 10461*

Abstract

Podocalyxin is a CD34-related sialomucin that is expressed at high levels by podocytes, and also by mesothelial cells, vascular endothelia, platelets, and hematopoietic stem cells. To elucidate the function of podocalyxin, we generated podocalyxin-deficient (*podxl*$^{-/-}$) mice by homologous recombination. Null mice exhibit profound defects in kidney development and die within 24 hours of birth with anuric renal failure. Although podocytes are present in the glomeruli of the *podxl*$^{-/-}$ mice, they fail to form foot processes and slit diaphragms and instead exhibit cell–cell junctional complexes (tight and adherens junctions). The corresponding reduction in permeable, glomerular filtration surface area presumably leads to the observed block in urine production. In addition, *podxl*$^{-/-}$ mice frequently display herniation of the gut (omphalocele), suggesting that podocalyxin may be required for retraction of the gut from the umbilical cord during development. Hematopoietic and vascular endothelial cells develop normally in the podocalyxin-deficient mice, possibly through functional compensation by other sialomucins (such as CD34). Our results provide the first example of an essential role for a sialomucin in development and suggest that defects in podocalyxin could play a role in podocyte dysfunction in renal failure and omphalocele in humans.

Key words: sialomucin • umbilical hernia • podocyte • hematopoiesis • vascular endothelium

Introduction

Podocalyxin (also called podocalyxin-like protein 1 [PCLP-1], Myb-Ets–transformed progenitor (MEP)21, and thrombomucin) is a heavily sialyated and sulfated membrane protein expressed on the apical surface of glomerular epithelial cells or podocytes and on vascular endothelia (1, 2). Although first described as a marker of podocytes and vasculature, podocalyxin expression has also been detected on mesothelial cells lining the coelomic cavity, platelets, and hematopoietic precursors cells (3–7). Recent experiments in avians and mice have shown that podocalyxin also marks the earliest detectable hematopoietic progenitors during development (5) as well as bipotent progenitors of blood cells and vascular endothelia called hemangioblasts (7).

Biochemical and sequence analysis have shown that podocalyxin is a 150–165-kD transmembrane protein composed of a mucin domain, a disulfide-bonded globular domain, a transmembrane region, and a highly charged cytoplasmic tail with potential phosphorylation sites for protein kinase C and casein kinase II (Fig 1). Structurally, it belongs to a large family of highly sulfated cell surface sialomucins of poorly understood functions. The amino acid sequence, protein structure, and genomic organization of podocalyxin suggest it is most closely related to two other molecules, CD34 and endoglycan (Fig. 1; references 5 and 8). CD34 is the prototypic member of this family and has been widely used in human and mouse as marker of hematopoietic progenitor cells and vascular endothelia (for a review, see reference 9). On high endothelial venules

R. Doyonnas and D.B. Kershaw contributed equally to this manuscript.

C. Duhme's present address is Green College Residence, University of British Columbia, Vancouver, BC, Canada.

Address correspondence to Kelly M. McNagny, Biomedical Research Centre, University of British Columbia, 2222 Health Sciences Mall, Vancouver, BC, Canada V6T 1Z3. Phone: 604-822-7810; Fax: 604-822-7815; E-mail: Kelly@brc.ubc.ca

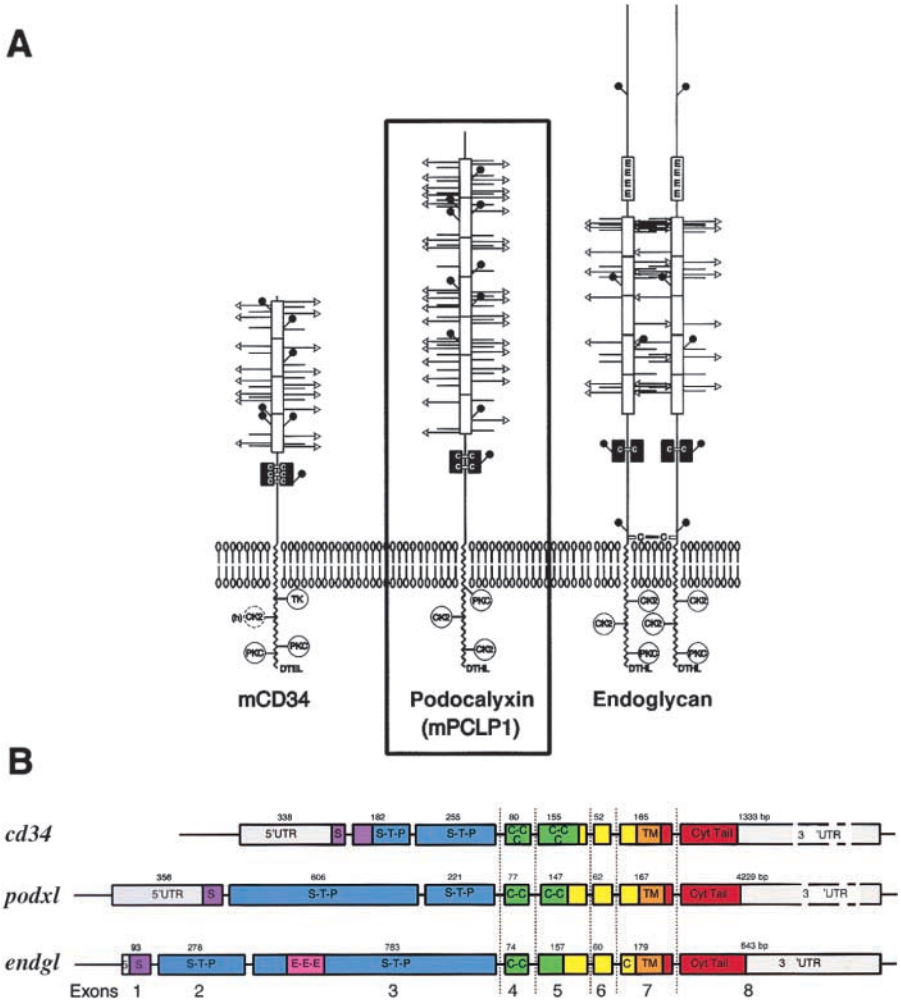

Figure 1. Protein structure and genomic organization of podocalyxin and the CD34 subfamily of sialomucins. (A) Schematic representation of the structure of murine CD34, podocalyxin, and endoglycan based on predicted protein sequences. White boxes, mucin domains; black boxes, cysteine-rich domains; circles, potential NH_2-linked carbohydrates; horizontal bars with or without arrows, potential *O*-linked carbohydrates; arrows, potential sialic acid motifs on *O*-linked carbohydrates; protein kinase C, TK, and CK2, potential phosphorylation sites; DTHL or DTEL, potential PDZ domain docking sites. (B) Schematic showing the genomic organization of human *cd34*, *podxl*, and *endgl* genes based on sequence contigs identified in the human sequence database (see Materials and Methods). The location of the coding sequences for the signal peptide (S, purple), mucin domain (S-T-P, blue), cysteine-rich domain (C-C, green), transmembrane (TM, orange), and cytoplasmic tail (Cyt tail, red) are indicated. Numbers indicate exon size in base pairs. The human cd34 gene spans ~25 kbp with a first intron of 11 kbp. The human *podxl* gene was found to span ~60 kbp with a first intron of 45 kbp. The human endgl gene spans >23 kbp with a first intron of 13 kbp. The 3′ introns of all three genes are relatively small; the last four exons in each case are separated by <3 kbp.

(HEVs)* CD34 (1) and podocalyxin (1) have been shown to act as an adhesive ligand for L-selectin expressed by leukocytes (10). This interaction requires HEV-specific glycosylation of CD34, and similar modifications have not been observed on the majority of vascular endothelial cells (ECs) or hematopoietic cells. Thus, it is remarkable that despite extensive use as a marker (>7,000 CD34-related publications), the functional role of CD34 on hematopoietic cells and most vascular cells remains obscure. Mice lacking CD34 develop normally (11, 12) although very subtle defects in hematopoietic maturation and function can be detected in in vitro assays or in in vivo assays of allergic responses. Endoglycan is the newest member of this gene family and has a broader distribution as it is expressed by hematopoietic progenitors and some mature blood cells, vascular endothelia, smooth muscle, and a subset of neuronal cells (13). Its function, too, is unknown.

Podocalyxin has been studied most extensively as a marker of kidney podocytes, which are epithelial cells that form a meshwork supporting the glomerular capillaries. The cellular architecture of podocytes can be described in three segments: the cell body, the major processes (MPs), and the foot processes (FPs; reference 14). The cell body and the MPs of the podocyte lie in the urinary space and are attached to the glomerular basement membrane (GBM) via the FPs. During glomerular development podocalyxin is first expressed on the apical surface of podocytes as they differentiate from epithelial precursors (15). Its expression then migrates laterally between cells and closely mirrors the appearance of open intercellular spaces between podocytes and the migration of occluding junctions down towards the basal surface of the podocyte. Close to this basal surface highly interdigitating FPs form and this is coupled to the modification of intercellular junctions to form slit diaphragms (SDs; reference 15). The slit diaphragm is a modified adherens junction (AJ) that defines the apical and basolateral surfaces of the mature podocyte FPs (16). During glomerular filtration, plasma is filtered through fenestrae in

**Abbreviations used in this paper:* AF, amniotic fluid; AJ, adherens junction; CD2AP, CD2-associated protein; EC, endothelial cell; ES, embryonic stem; FP, foot process; GBM, glomerular basement membrane; GLEPP, glomerular epithelial protein; HEV, high endothelial venule; HPRT, hypoxanthine-guanine phosphoribosyl transferase; JC, junctional complex; KO, knockout; MP, major process; NPHS, congenital nephrotic syndrome; PECAM, platelet endothelial cell adhesion molecule; SD, slit diaphragm; TEM, transmission electron microscopy; TJ, tight junction.

the capillary endothelium and then through the GBM. In the final stage of ultrafiltrate production the filtrate passes through the SDs between the interdigitating FPs. On mature podocytes, podocalyxin is a major component of the apical cell surface where it has been proposed to help maintain the spacing between the interdigitating FPs by charge repulsion (15). The proper function of podocytes as filters is critically dependent on the anionic nature of the glycocalyx covering the podocytes (17–19). In the 1970s it was shown that neutralization of this charged glycocalyx by infusion of polycations, or by treatment with glycosidases to remove negatively charged carbohydrates, results in a rapid remodelling of the podocyte cytoskeleton with "effacement" or loss of the fine, interdigitating FP structure and SDs. This, in turn, resulted in nephrosis and massive proteinuria (17–19). With the later discovery that podocalyxin is the most abundant heavily charged sialomucin expressed by podocytes, it was speculated that alterations in podocalyxin could be the principal cause of these experimentally induced nephrotic syndromes (1, 2).

Although mutations in the podocalyxin gene have not yet been linked to nephrotic syndrome and renal failure, several other human and murine gene mutations of podocyte proteins have been identified. These include mutations in nephrin/congenital nephrotic syndrome (NPHS) gene 1, podocin/NPHS gene 2, α-actinin-4, CD2-associated protein (CD2AP), and $\alpha_3\beta_1$ integrin (20–24). Although the precise function of the proteins encoded by several of these genes is uncertain they have one common denominator: their mutation leads to the disruption of normal podocyte architecture (25–27).

To determine whether podocalyxin plays an essential role in renal, vascular, and hematopoietic function we have disrupted the podocalyxin-encoding gene in mice (*podxl*$^{-/-}$). All *podxl*$^{-/-}$ mice die within the first 24 h of postnatal life from profound defects in kidney and/or gut formation (herniation or omphalocele). Surprisingly, the loss of podocalyxin expression did not result in the massive proteinuria characteristic of leaky podocyte filtration in human nephrotic syndromes. Instead, newborn *podxl*$^{-/-}$ mice were anuric (no measurable urine in the bladder) and failed to form FPs and SDs. Our data suggest that podocalyxin is indispensable for normal murine development and that its mutation could play a role in podocyte-related renal failure and in omphalocele (see Discussion).

Materials and Methods

Genomic Structure and Peptide Motif Analyses. The 8 exons of *cd34*, *podxl*, and *endgl* genes were found by sequence analysis and database searches. Human *cd34* cDNA (GenBank/EMBL/DDBJ accession no. M81104) was used to identify the human genomic locus on clone 8L2 of chromosome 1q32.2-q32.3 (GenBank/EMBL/DDBJ accession no. AL035091). Human *podxl* cDNA (GenBank/EMBL/DDBJ accession no. NM005397) was aligned with the working draft sequence of human chromosome 7 clone RP11-180C16 (GenBank/EMBL/DDBJ accession no. AC008264), and human *endgl* cDNA (GenBank/EMBL/DDBJ accession no. AF219137) was aligned against the working draft sequence of human chromosome 15 clone RP11-221C9 (GenBank/EMBL/DDBJ accession no. AC023593). For structural predictions of CD34, podocalyxin, and endoglycan, potential *O*-linked glycosylation sites were predicted using the www.cbs.dtu.dk/services/NetOGlyc server, and potential phosphorylation sites were predicted using subsequence analysis of protein patterns in MacVector (Oxford Molecular).

Targeted Disruption of the Podocalyxin (podxl) Gene. A partial mouse podocalyxin cDNA clone (534 bp) was produced by reverse transcription PCR of mouse kidney RNA using primers to the 3′-coding sequence of chicken podocalyxin: 5′-GAATTCGGCTTCTCGTGGAACTGCTGTGTCACT-3′ and 5′-GAATTCGGCTTCTCCTCATCTAGGTCATCCTTGG-3′. This probe was used to screen a 129/SvJ phage library in λFIXII (Stratagene), and 3 independent mouse *podxl* genomic clones were identified and purified. A mutant allele of the *podxl* genomic locus was generated by inserting a neomycin resistance cassette in the antisense orientation between the XbaI site in exon 5 and an engineered XhoI site in exon 8 of the m-*podxl* gene, thereby deleting the majority of exons 5, 6, 7, and 8. The 5.5-kb XbaI fragment containing part of the 5th exon was subcloned into the XbaI site of the pPNT vector (28) to create the 5′ arm of homology in the knockout (KO) vector (29, 30). The 3′ arm of homology was created by PCR of an 892-bp fragment from the 3′ region of the MEP21 coding sequence using primers 5′-GCGGCCGCTTACTAGGCATGGTTTTATG-3′ and 5′-CTCGAGACACCTCTGATCTGTCTGCTGGTC-3′, and this was cloned into the NotI and XhoI sites of pPNT. The resulting vector was electroporated into E14 embryonic stem (ES) cells and these were selected for resistance to G418 and against sensitivity to ganciclovir. Of 672 resistant ES cell clones, 384 were screened by Southern blot analysis for presence of a 5-kb HindIII fragment using the strategy depicted in Fig. 2. Blastocyst injection of these ES cells and production of germline transmitting chimeras was performed by RCC Ltd., using standard protocols. Genomic DNA from mouse tail cuts or tissue samples was isolated using the DNAeasy Tissue Kit (QIAGEN). Genotypes were determined by PCR using wild-type and KO specific primers (5′-AGTGAGAGACACATTGGGTAACT-3′ wild-type allele specific, 5′-TATCGCCTTCTTGACGAGTTCTT-3′ KO allele specific, and 5′-GAGGATTTGTGCACTCTACATGTG-3′ common primer; GIBCO BRL). The wild-type allele resolves as a 760-bp band, while the KO allele resolves as a 550-bp band.

Nucleic Acid Analyses. All hybridization probes were labeled with [^{32}P]dCTP by random hexamer priming as described by Feinberg and Vogelstein (31). For Southern blot analyses, ES cell clones were grown in 48-well plates. Cells were lysed and genomic DNA was ethanol precipitated and digested with HindIII in the plates using standard protocols (32). DNA samples (~40 μg per sample) were resolved on 0.7% agarose gels, denatured with NaOH, and transferred to nylon membranes. Membranes were hybridized with radiolabeled probes corresponding to the 2,200-bp ApaI fragment of the podocalyxin 3′ untranslated region (see Fig. 2). Hybridization of radiolabeled probes and removal of unbound probe was performed in $NaHPO_4$/SDS buffer as described by Church and Gilbert (33). In this assay, the wild-type *podxl* locus resolves as a 4-kb HindIII fragment while the homologously recombined locus resolves as a diagnostic 5-kb fragment.

For Northern blot analysis, total RNA was prepared by lysis and fractionation in guanidinium/acetate/phenol/chloroform as described by Chomczynski and Sacchi (34). Approximately 10 μg of each RNA was resolved on a 1% agarose-formaldehyde gel

and blotted onto nylon membranes (GeneScreen; Dupont). [^{32}P]-labeled probes were generated from the 490-bp SmaI-HindIII fragment encoding the mucin domain of the mouse podocalyxin cDNA or from a 1,000-bp PstI fragment of the glyceraldehyde-3-phosphate dehydrogenase cDNA as a control for RNA loading (35).

Histological Analyses and Immunohistochemistry. Immunoperoxidase staining of snap frozen embryo tissues was performed using anti-PCLP-1 antibody (7), anti-CD34-biotin (BD PharMingen), and anti-CD31 (platelet endothelial cell adhesion molecule [PECAM]-1; BD PharMingen), followed by Vector Elite developing reagents (Vector Laboratories) and methyl green counterstain, as described previously (5). For paraffin sections, embryonic day 19 kidneys were fixed in 10% formalin, embedded in paraffin, and sectioned. After deparafinization and hydration the tissue sections were treated with target unmasking fluid (Signet Labs) for 16 h at 90°C (34) and stained with monoclonal antibodies to glomerular epithelial protein (GLEPP)1, nephrin, or control rat IgG. Antibody binding was revealed by staining with biotinylated goat anti–rat antibodies, followed by streptavidin-peroxidase, and 3,3′-diaminobenzidine–developing reagent using ABC reagents and protocols from Vector Laboratories. Sections were counterstained with periodic acid-Schiff's reagent using standard protocols (3). Immunofluorescence staining was performed essentially as described previously (36). Cryostat sections of mouse E19 kidneys were fixed in acetone and incubated with blocking solution (10% goat or donkey serum in PBS). Primary antibodies used were chicken anti–mouse GLEPP1 (courtesy of Dr. Roger Wiggins, University of Michigan, Ann Arbor, MI); rabbit anti–mouse nephrin (courtesy of Dr. Lawrence Holzman, University of Michigan); rabbit anti–mouse collagen α4(IV) and laminin α5 (courtesy of Dr. Jeff Miner, Washington University School of Medicine, St. Louis, MO); mouse monoclonal anti-synaptopodin (courtesy of Peter Mundel, Albert Einstein College of Medicine, Bronx, NY); rabbit anti–human Wilm's tumor protein 1 (Santa Cruz Biotechnology, Inc.); rat anti–mouse PECAM-1 (BD PharMingen); and rat anti–mouse laminin, laminin β1 and β2 (Chemicon International). For collagen α4(IV) staining, sections were pretreated with 6 M urea, 0.1 M glycine for 1 h at 4°C (37). Secondary antibodies were FITC-conjugated goat anti–rat (Southern Biotechnology Associates, Inc.), Cy3-conjugated goat anti–rabbit (Jackson ImmunoResearch Laboratories), FITC-conjugated goat anti–mouse (Cappel), and FITC-conjugated donkey anti–chicken (Lampire Biological Laboratories). All incubations were carried out in blocking solution. A Nikon Diaphot microscope and a Hamamatsu digital camera were used for acquisition of immunofluorescence images.

Transmission Electron Micrographs. For transmission electron micrographs (TEMs), newborn kidneys were fixed in cold glutaraldehyde/cacodylate buffer. After plastic embedding, one micron sections were stained with toluidine blue. Selected samples containing glomeruli were thinly sectioned, stained with uranyl acetate, and examined by TEM as described previously (38). The most mature glomeruli on the sections with open capillary loops and urinary spaces were examined.

Flow Cytometric Analysis. For single color, indirect immunofluorescence analysis, 10^6 cells from fetal liver, spleen, or bone marrow were preincubated with Fc block (anti-mCD16/32. clone 2.4G2; reference 39) in PBS containing 10% FCS and 0.05% azide. These cells were then stained with either biotin-, FITC-, or phycoerythrin-conjugated monoclonal antibodies to CD34 (40), Sca-1 (41), c-kit (42), CD41, Mac1 (43), B220 (44), CD3 (45), CD4 (46), CD8 (47), or with unlabeled antibodies to Ter119 (48), Gr-1 (49), or PCLP-1 (7) followed by goat anti–rat-FITC-coupled or biotin-coupled secondary antibodies (BD PharMingen) as described previously (50). All flow cytometric analyses were performed using a FACScan™ (Becton Dickinson).

Blood, Urine, and Amniotic Fluid Analysis. Newborn mice were left for 30 min under a heating lamp and then killed by decapitation. Blood was collected from the aorta in 50-μl heparinized capillary tubes, and urine was collected in 5-μl capillary tubes after gentle massage of the bladder. The volume of urine produced from each mouse was measured and a 2-μl sample was analyzed for protein content by 10% SDS-PAGE under nonreducing conditions. After electrophoresis, proteins were visualized by silver staining. Blood samples were clotted and serum was analyzed for their creatinine/urea content using a modified creatinine kit (Sigma-Aldrich). Amniotic fluid was collected at 15 d after coitum and 1 μl of unconcentrated amniotic fluid was analyzed by 10% SDS-PAGE. As an indirect measure of blood pressure, day 18 embryos were rapidly dissected and placed in 1 ml of PBS with 1 mM EDTA. The umbilical cord was severed and embryonic blood was allowed to flow freely for 60 s. The cord was then clamped, the embryo and placenta were removed, and the number of RBCs released into the PBS was counted.

Results

Generation of Podocalyxin-Deficient Mice. To address the role of podocalyxin in kidney, vascular and hematopoietic development we generated podocalyxin-deficient mice by homologous recombination (*podxl*$^{-/-}$, Figs. 1 and 2; reference 28). The *podxl* recombination vector was designed to delete the majority of the coding sequence for exons 5, 6, 7, and 8, and replace them with the neomycin-resistance gene in the antisense orientation (Fig. 2 A). These exons encode 55 amino acids in the extracellular/juxtamembrane region, the transmembrane region, and the entire cytoplasmic tail of podocalyxin and represent the most highly conserved domains across species (5, 7, 8). The vector was transfected into E14 ES cells and 384 G418 and ganciclovir-resistant clones were screened for homologous recombination by Southern blot analysis (Fig. 2 B). 16 clones were identified with the appropriate recombination and four were injected into blastocysts. Of the four ES cell clones, one gave >90% chimerism in six of the resulting offspring and all of these mice transmitted the targeted allele to their progeny, as determined by PCR analysis (Fig. 2 B). These were backcrossed for more than five generations onto both Balb/c and C57BL/6 backgrounds. Sibling crosses to generate wild-type (*podxl*$^{+/+}$), heterozygous (*podxl*$^{+/-}$), and KO mice (*podxl*$^{-/-}$) consistently yielded offspring of similar phenotype in both genetic backgrounds.

To confirm that podocalyxin expression had been ablated in *podxl*$^{-/-}$ mice, Northern blot analysis was performed with RNA isolated from 16-d fetal lungs of *podxl*$^{+/+}$, *podxl*$^{+/-}$, and *podxl*$^{-/-}$ embryos, using the 5′ region encoding the podocalyxin extracellular domain (lying outside the region of recombination) as a probe (Fig. 2 C). This analysis revealed the presence of the expected 5-kb podocalyxin transcript in wild-type embryos, reduced expression in heterozygote, and a complete lack of hybridiz-

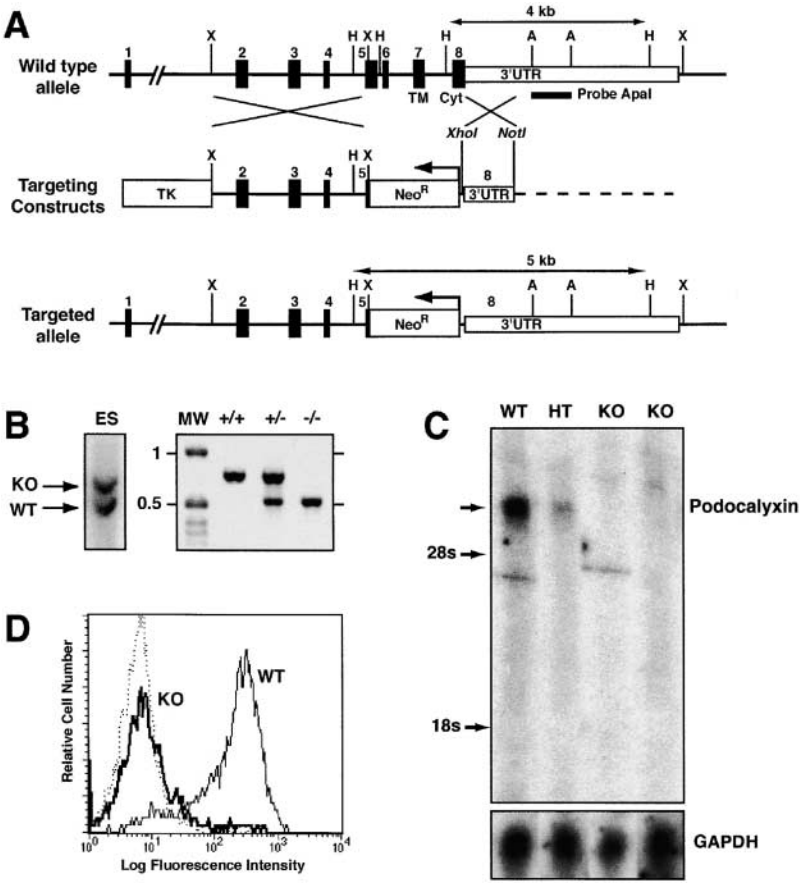

Figure 2. Generation of podocalyxin-null mutation in mice. (A) Scheme showing structure of mouse podocalyxin genomic locus, targeting construct, and the predicted homologous recombination event. The targeted disruption results in the deletion of the majority of exons 5, 6, 7, and 8 encoding the 55 amino acids of the juxtamembrane ("stalk") domain, the transmembrane region (TM), and the cytoplasmic tail (Cyt). These were replaced with the neomycin resistance cassette (Neo^R) in the antisense orientation. Southern blot probe, restriction sites, and predicted sizes of targeted and wild-type alleles (HindIII digest) are indicated. (B) Southern blot and PCR analysis of podocalyxin gene in targeted ES cell clones and chimeric mice. ES lane shows a Southern blot of a mutant ES cell clone used to generate $podxl^{-/-}$ mice. The indicated 2.2-kbp ApaI fragment was used as probe. 4-kbp wild-type (WT) and 5-kb mutant (KO) alleles are indicated. Genomic DNA from wild-type (+/+), heterozygous (+/−), and homozygous KO mice (−/−) were analyzed by PCR using allele-specific primers (see Materials and Methods). Molecular weight markers (MW) are indicated in kbp. (C) Northern blot analysis of 16-d embryo lung RNA from wild-type (WT), $podxl^{+/-}$ (HT), and $podxl^{-/-}$ (KO) mice. 10 μg of total RNA per lane was hybridized with probes specific to the mucin domain of podocalyxin or glyceraldehyde-3-phosphate dehydrogenase as a control. (D) Analysis of podocalyxin expression by 15-d fetal liver cells. Single cell suspensions from wild-type (WT) and $podxl^{-/-}$ (KO) mice were stained with anti–PCLP-1 antibody followed by FITC-conjugated goat anti–rat antibodies before flow cytometry analysis. Fetal liver cells were gated on forward and side scatter to focus on the MEP21 expressing subpopulation of fetal liver.

ing transcripts in $podxl^{-/-}$ embryos suggesting a loss of expression from the targeted allele. This was confirmed at the protein level by cell surface immunofluorescence analysis of 15-d fetal liver cells using a monoclonal antibody to mouse podocalyxin (Fig. 2 D). Hematopoietic cells from $podxl^{+/+}$ and $podxl^{+/-}$ mice expressed high levels of podocalyxin on their surface, while $podxl^{-/-}$ showed no reactivity. From these analyses we conclude that the engineered rearrangement in the podocalyxin locus has resulted in a complete loss of podocalyxin expression in $podxl^{-/-}$ mice.

Perinatal Lethality, Omphalocele, and Edema in $podxl^{-/-}$ Mice. PCR and Southern blot analyses of 6-wk-old progeny from heterozygous crosses between $podxl^{+/-}$ mice revealed the complete absence of any $podxl^{-/-}$ offspring suggesting embryonic or perinatal lethality in mice lacking podocalyxin. To more accurately pinpoint the time of disappearance, embryos were harvested at various stages of development and genotyped by PCR. Although we observed the expected Mendelian frequency of $podxl^{+/+}$, $podxl^{+/-}$, and $podxl^{-/-}$ offspring throughout embryonic development, all $podxl^{-/-}$ mice died within the first 24 h of postpartum life (Table I). No statistically significant differences were observed in the birth weight of $podxl^{+/+}$ newborns and their $podxl^{-/-}$ littermates. Likewise, no significant differences were noted in the organ weight or macroscopic appearance of the lungs, liver, heart, gut, and kidneys of the majority of the $podxl^{-/-}$ mice (although two notable defects were observed in a subset of the $podxl^{-/-}$ mice, see below). Perinatal lethality persisted when $podxl^{-/-}$ mice were delivered by Caesarean section and placed with foster mothers. Thus, the data

Table I. *Frequency of $podxl^{+/+}$, $podxl^{+/-}$, and $podxl^{-/-}$ Embryos during Development*

	Number of animals/genotype			
Age of embryos (post coitum)	+/+	+/−	−/−	Frequency of −/− mice
				%
15 d	19	28	17	26
16 d	5	21	10	27
17 d	8	15	10	30
18 d	35	71	30	22
19 d	6	10	8	33
Age of newborn (post partum)				
1 d	52	100	0	0

Embryos from timed matings were genotyped on embryonic day 15, 16, 17, 18, 19, or 1 d post partum. Far right column shows the observed percentage of $podxl^{-/-}$ mice (the predicted Mendelian percentage is 25%).

suggest that the loss of podocalyxin results in perinatal lethality due to defects intrinsic to *podxl*$^{-/-}$ mice.

Although the majority of newborn *podxl*$^{-/-}$ mice displayed no overt defects, two significant anomalies were observed in a subset of these mice: edema and omphalocele. Careful analysis of the embryos obtained by Caesarean section shows that ~25% of the *podxl*$^{-/-}$ embryos (3/12 at embryonic day 18 and 4/15 at embryonic day 15) exhibited mild to severe edema. This usually appeared as subdermal swelling as early as 15 d after coitum (Fig. 3) and a mildly turgid trunk and appendages at day 18 (data not shown). More strikingly, ~30% of all *podxl*$^{-/-}$ mice were born with an "omphalocele" or herniation of the gut into the umbilical cord (Fig. 4, A and B). No direct correlation was observed between embryonic edema and omphalocele; *podxl*$^{-/-}$ embryos at day 18 were equally likely to have one, the other, or both defects. However, neither defect was ever observed in any day 18 *podxl*$^{+/+}$ or *podxl*$^{+/-}$mice suggesting a strict correlation with podocalyxin loss.

Omphalocele is a normal physiologic process that occurs transiently during the embryogenesis of all mammals. It is known that at midgestation, the rapidly enlarging visceral organs soon exceed the limiting space of the peritoneal cavity. As a result, the developing gut herniates into the umbilical space (this begins at embryonic day 12 in mice; reference 51). Normally this "physiologic omphalocele" is resolved by the subsequent expansion of the peritoneal cavity and retraction of the gut from the umbilical cord. In mice, this retraction is completed by the 16th day of embryonic development (51). To assess the ontogeny of gut herniation in podocalyxin-deficient mice, timed matings were performed and *podxl*$^{+/+}$, *podxl*$^{+/-}$, and *podxl*$^{-/-}$ embryos were evaluated at daily intervals for the presence or absence of omphalocele (Fig. 4 D). As expected, wild-type embryos showed a complete resolution of the physiologic omphalo-

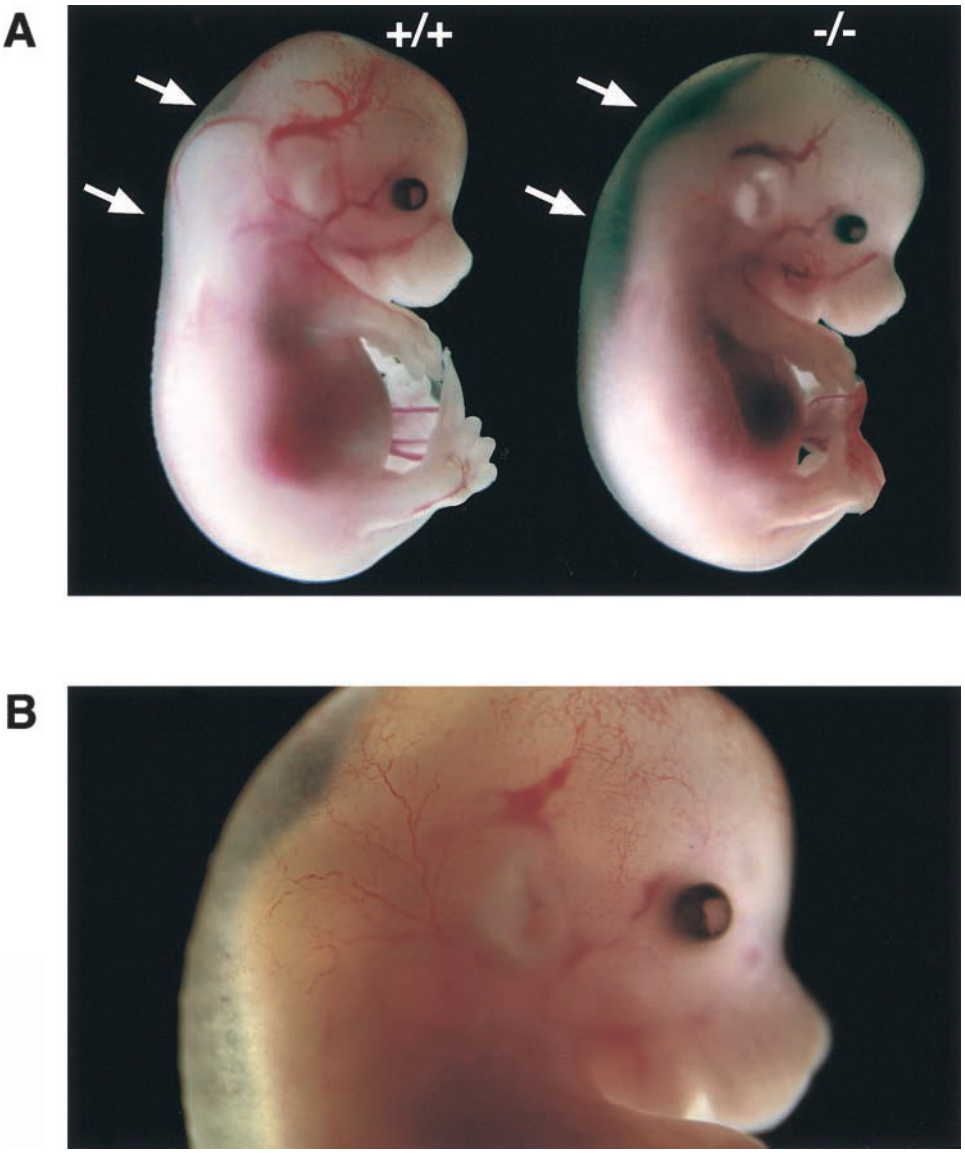

Figure 3. Edema. (A) Light micrograph of day 15 *podxl*$^{+/+}$ (+/+) embryo and one of a *podxl*$^{-/-}$ (−/−) embryo with edema. (B) Close-up color micrograph of day 15 *podxl*$^{-/-}$ embryo with edema. Arrows indicate the dorsal region of embryonic trunk where subdermal swelling occurs in −/− embryos.

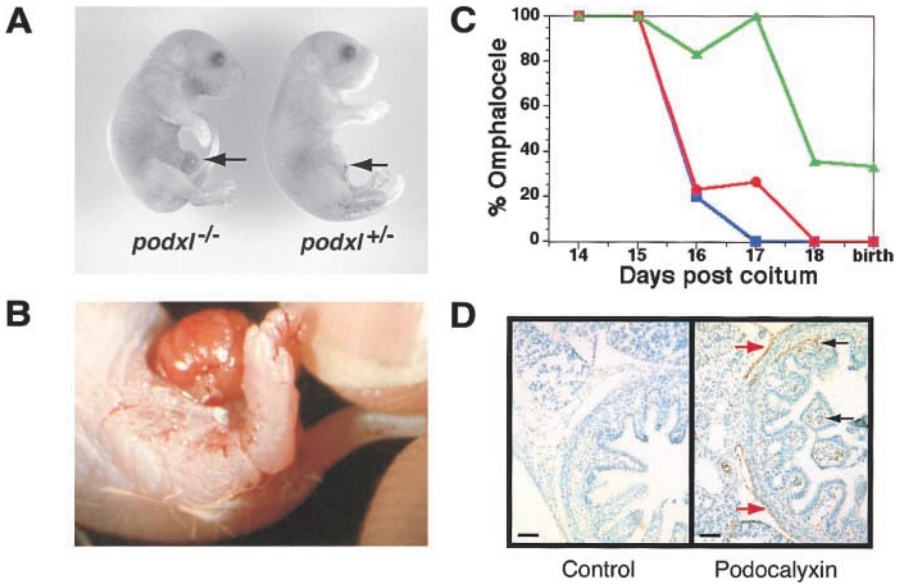

Figure 4. Omphalocele. (A) Light micrograph of day 18 *podxl*$^{+/+}$ and *podxl*$^{-/-}$ embryos. Arrow indicates umbilical cord and omphalocele. (B) Close-up color micrograph of omphalocele in *podxl*$^{-/-}$ newborn. (C) Ontogeny of omphalocele in wt, *podxl*$^{+/-}$, and *podxl*$^{-/-}$ mice. Blue, red, and green symbols indicate wt, *podxl*$^{+/-}$, and *podxl*$^{-/-}$ mice, respectively. Each data point represents the percentage of between 5 and 35 animals analyzed. (D) Analysis of podocalyxin expression in physiologic omphalocele of wild-type mice. Sections from 16-d embryo gut were immunostained for podocalyxin (brown stain) and counterstained with methyl green. Podocalyxin is expressed by mesothelial cells lining the outer aspect of the gut (red arrows) and by capillary ECs in the villi (black arrows).

cele by embryonic days 15 or 16. In contrast, virtually all *podxl*$^{-/-}$ embryos (13/14) displayed omphalocele up to embryonic day 17. Subsequently (and before birth), 70% of these mice resolved the omphalocele resulting in a 30% incidence in newborns. *podxl*$^{+/-}$ mice displayed an intermediate phenotype (8/35 displayed omphalocele on day 17), suggesting partial impairment due to loss of one *podxl* allele (Fig. 4 C). This phenotype may be linked to the prominent expression of podocalyxin on mesothelial cells lining the serous body cavities (Fig. 4 D). Thus, although omphalocele is only observed in a subset of neonates, the data suggest that all podocalyxin-deficient mice (and a subset of heterozygotes) present with some degree of abnormal omphalocele during development.

Podocalyxin Deficiency Leads to Symptoms Consistent with Neonatal Anuric Renal Failure. The observation that only a subset of newborn *podxl*$^{-/-}$ have overt defects, and yet 100% of these mice die perinatally prompted us to perform more detailed analyses of organ function in these mice. Since podocalyxin is most prominently expressed in kidneys, we aspirated bladder contents to analyzed urine from newborns. Strikingly, 100% of the *podxl*$^{-/-}$ newborns (12/12) exhibited a lack of urine in the bladder suggestive of severely impaired kidney function (Fig. 5 A). Consistent with anuria (and not proteinuria) SDS-PAGE analysis of blood serum and amniotic fluid proteins showed no significant differences in protein constituents from wild-type and KO mice. Anuria is one of several clinical features of acute renal failure and can lead to intravascular volume expansion and hypertension. Other symptoms include increased blood pressure and elevated levels of serum creatinine and urea. Although direct measurement of blood pressure was not possible in newborn mice, we attempted to measure this indirectly by assessing cardiac output. Day 18 embryos were collected by Caesarean section, the umbilical cord of each embryo was severed and the RBCs were collected in a solution of PBS/EDTA for 60 s. These were then counted as a rough measure of cardiac output/blood pressure (Fig. 5 B). While no significant differences were observed between *podxl*$^{+/+}$ and *podxl*$^{+/-}$ embryos, *podxl*$^{-/-}$ embryos exhibited an ~15-fold increase in released RBCs over the 60-s interval (most were released within the first 15 s). Consistent with this observation, *podxl*$^{-/-}$ embryos frequently appeared pale when the umbilical cords were severed in solutions that prevented clotting. This did not reflect an inability to clot as no differences in pallor were observed when the umbilical cords were severed in the absence of aqueous anti-coagulants, and we have not observed any differences in the frequency or function of platelets in *podxl*$^{-/-}$ mice (see below). An increase in blood pressure may offer an explanation for the edema observed in *podxl*$^{-/-}$ embryos: excessive pressure could drive fluid into the extravascular spaces. Although there were no significant differences in serum creatinine/urea levels between wild-type and *podxl*-deficient mice, it is likely that such changes would only appear after 1 or 2 d of life postpartum (during embryogenesis these would be removed maternally). Newborn mice with anuric renal failure have been described to consistently die in the first day of life (52–55), and thus it is likely that *podxl*$^{-/-}$ mice die due to kidney failure.

Podocalyxin Is Required for Normal Formation of Podocyte FPs in Developing Kidneys. To more clearly define the defects in *podxl*$^{-/-}$ kidneys, we examined glomerular development in wild-type and *podxl*$^{-/-}$ animals. Periodic acid-Schiff staining of sections from newborn kidney revealed the presence of glomeruli in all stages of development in both *podxl*$^{-/-}$ and *podxl*$^{+/+}$ mice but with subtle differences. In some of the mature juxtamedullary glomeruli of the *podxl*$^{-/-}$ kidneys lucent areas (vacuoles) were observed which were distinct from the normal capillary loops (Fig. 6 A, and data not shown). During embryogenesis the onset of podocalyxin expression correlates with early podocyte differentiation from mesenchymal progenitors at the "S-shaped body" stage of glomerular development (15). To

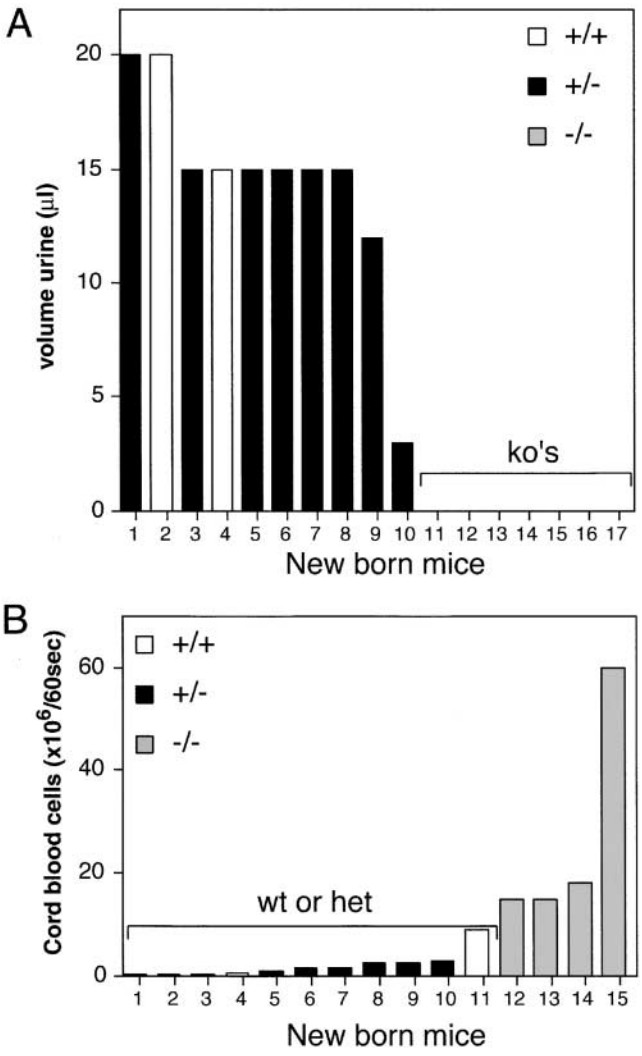

Figure 5. Urine production and cardiac output. (A) Urine collected from the bladders of 18-d-old embryos after Caesarian section. Representative data from one of two similar experiments. White bars, wild-type embryos; black boxes, *podxl*$^{+/-}$ embryos; gray boxes, *podxl*$^{-/-}$ embryos. (B) 60-s cardiac output from 18-d-old embryos as determined by RBCs released from umbilical cord. White bars, wild-type embryos; black boxes, *podxl*$^{+/-}$ embryos; gray boxes, *podxl*$^{-/-}$embryos.

determine whether podocalyxin loss results in a failure of podocyte maturation, kidneys from newborn mice were sectioned and analyzed by immunohistochemistry for expression of two later markers of podocyte differentiation: GLEPP1, a transmembrane tyrosine phosphatase of kidney podocytes (56) and nephrin, a transmembrane protein associated with podocyte SDs that plays a critical role in podocyte function (20, 57). Wild-type, *podxl*$^{+/-}$, and *podxl*$^{-/-}$ kidneys all displayed the expected GLEPP1 and nephrin staining on podocytes in the glomeruli (Fig. 6 A, and data not shown), indicating that podocyte differentiation and expression of these maturation markers is not impaired by the lack of podocalyxin. However, the morphology of the podocytes was clearly altered in *podxl*$^{-/-}$ mice: consistent with the periodic acid-Schiff stains, distinct lucent areas suggestive of void spaces and vacuoles were observed within the podocytes of *podxl*$^{-/-}$ mice (Figs. 6 A and 7 A). To ensure that this was due to alterations intrinsic to the podocytes and not to alterations in protein expression by the vascular ECs or GBMs, dual-label immunofluorescence analysis was performed with vascular/GBM markers (PECAM-1, collagen α4(IV), and laminins α5, β1, and β2) and podocyte markers (Wilm's tumor gene product [58], GLEPP1 [56], nephrin [20, 57], and synaptopodin [59]). We found no evidence of loss of expression of any GBM proteins in wild-type and *podxl*$^{-/-}$ kidneys (Fig. 6, and data not shown). The mature glomeruli of the newborn *podxl*$^{+/+}$ and *podxl*$^{-/-}$ mice showed similar expression levels of collagen and laminin isoforms in mature GBM (Fig. 6, B and C, and data not shown). Normally, podocyte FP and GBM proteins appear to have an overlapping staining pattern at the light microscopy level. This reflects the fact that the thin FPs of podocytes are in very close proximity to the GBM rather than true "colocalization". Interestingly we noted a consistent reduction in the degree of "side-by-side" podocyte and GBM-marker staining in *podxl*$^{-/-}$ kidneys. For example, while dual immunofluorescence-labeling showed the normal close proximity of the podocyte markers nephrin and GLEPP1 with the GBM in wild-type mice (note the red/green proximity in Fig. 6, B and C), there was a marked decrease in the degree of overlap in the *podxl*$^{-/-}$ glomeruli. This indicates either a greater-than-normal distance between the podocyte apical membranes and the GBM (cell thickening) or incomplete coverage of the basement membranes by podocyte FPs.

To assess the defects in the *podxl*$^{-/-}$ podocytes more precisely, kidneys were analyzed by TEM. TEM of the most mature glomeruli from newborn *podxl*$^{+/+}$ and *podxl*$^{+/-}$ mouse kidneys showed well-developed MPs and FPs (Fig. 7 A, and schematic in Fig. 8). By contrast, in the *podxl*$^{-/-}$ kidneys, MPs were greatly reduced in number and the FPs and SDs were completely absent. Interestingly, numerous junctional complexes (JCs) (tight junctions [TJs] and AJs) were observed between adjacent podocytes (Fig. 7, A and B) consistent with impermeable cell–cell junctions. Moreover, the podocytes in *podxl*$^{-/-}$ mice completely engulf the vasculature with their cell bodies and the urinary spaces were markedly reduced. Consistent with light microscopic observations (see above) large intracellular vacuoles were present in the podocytes of *podxl*$^{-/-}$ mice (Figs. 6 A and 7 A). On the endothelial side of the GBM the ECs had some, but fewer, fenestrae and in general the EC layer appeared thicker than in wild-type mice (Figs. 7 and 8). These ultrastructural findings are consistent with the lack of urine production in *podxl*$^{-/-}$ mice and this is most likely cause of death in podocalyxin-deficient mice (Fig. 8).

Vascular Development. Since podocalyxin is also expressed on vascular ECs we next examined the distribution of these cells in whole-mount sections of 16-d *podxl*$^{+/+}$ and *podxl*$^{-/-}$ embryos by immunocytochemistry. Stains of embryos with CD31 (PECAM-1) and CD34 antibodies show no detectable differences in the expression pattern of

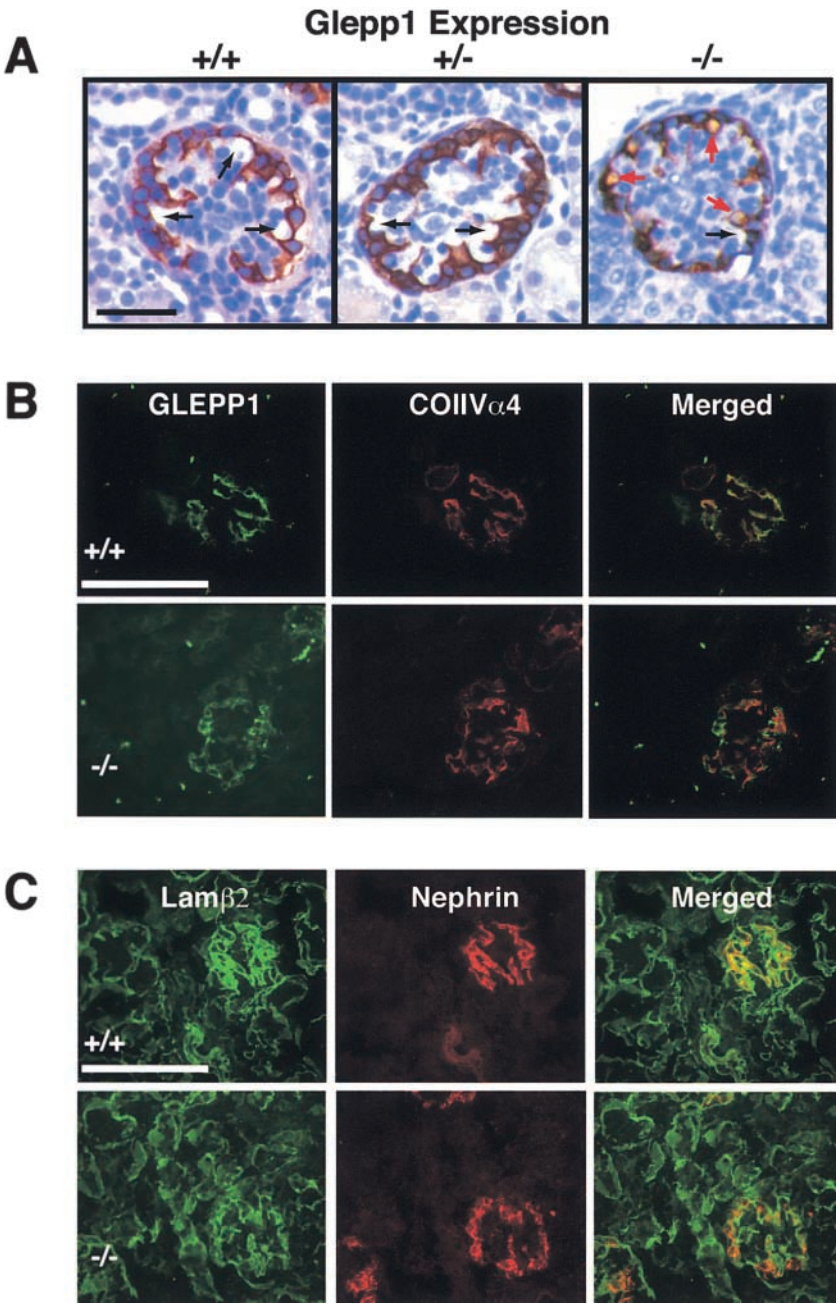

Figure 6. Histological analysis of *podxl*$^{-/-}$ kidneys. (A) Immunohistological analysis of expression of the podocyte-specific tyrosine phosphatase, GLEPP1 in *podxl*$^{+/+}$, *podxl*$^{+/-}$, and *podxl*$^{-/-}$ kidneys. The capillary loops of the *podxl*$^{+/+}$ and *podxl*$^{+/-}$ glomeruli are shown in black arrows. *podxl*$^{-/-}$ glomeruli had similar capillary loops but also had numerous lucent vacuoles surrounded by GLEPP1 staining (red arrows). Scale bars, 50 μm. (B) Dual-label indirect immunofluorescence of newborn mouse kidney from *podxl*$^{+/+}$ and *podxl*$^{-/-}$ (top and bottom, respectively) with antibodies to GLEPP1 (donkey anti-chicken FITC labeled secondary antibody), and collagen α4 (type IV) (goat anti–rabbit Cy3-labeled secondary antibody). Staining for the apical membrane podocyte marker GLEPP1 and the basement membrane protein collagen α4 (type IV) is seen in mature glomeruli in *podxl*$^{+/+}$ and *podxl*$^{-/-}$ mice. Superimposition of these images shows areas of strong overlap (orange) in the *podxl*$^{+/+}$ mice. In the *podxl*$^{-/-}$ mice the area of overlap (orange) is diminished representing a greater distance in the localization of the apical membrane marker (GLEPP1) from the basement membrane. (C) Dual-label indirect immunofluorescence of newborn mouse kidney from *podxl*$^{+/+}$ and *podxl*$^{-/-}$ (top and bottom, respectively) with antibodies to the basement membrane protein laminin β2 (FITC-conjugated goat anti–rat) and podocyte slit diaphragm protein nephrin (anti–rabbit Cy3-labeled secondary antibody). Strong staining is seen for both markers in *podxl*$^{+/+}$ and *podxl*$^{-/-}$ mice. The close proximity of the slit diaphragm (nephrin staining) to the basement membrane (laminin β2 staining) can be appreciated in the superimposed images by the presence of overlapping staining (orange) in the *podxl*$^{+/+}$ mice. In the *podxl*$^{-/-}$ glomeruli the superimposed images show diminished overlap (orange staining) of the expression of nephrin and laminin β2.

these molecules between *podxl*$^{+/+}$ and *podxl*$^{-/-}$ in brain, gut, kidney, or lung. However, a consistent increase in the expression levels of CD34 was detected particularly in kidney and lung (Fig. 9 A, and data not shown). Quantification of CD34 mRNA from kidney revealed a three to fourfold increase in CD34 transcripts in *podxl*$^{-/-}$ mice versus *podxl*$^{+/+}$ mice (Fig. 9 B), while the frequency of control hypoxanthine-guanine phosphoribosyl transferase (HPRT) mRNAs were found to be identical in null and wild-type mice. This result suggests that a loss of podocalyxin expression by the vasculature may result in a compensatory increase in the expression of the related sialomucin, CD34. Consistent with normal vasculature in areas of CD34/podocalyxin coexpression, TEM analyses of newborn lungs from podocalyxin-deficient mice revealed no overt defects in formation of pulmonary capillaries or bronchial-associated epithelia (data not shown). Unfortunately, the third member of the CD34 family, endoglycan, is expressed by a variety of nonvascular cell types making the assessment of its upregulated expression on vessels problematic (unpublished data, and reference 13). We conclude that the vascular development in *podxl*$^{-/-}$ mice is essentially normal, possibly due to the upregulated expression of the related molecule, CD34.

Hematopoietic Development is Normal in podxl$^{-/-}$ *Embryos.* Because our own previous studies in the chick (5, 50) and recent studies in the mouse (7) have shown that podocalyxin is a marker of the earliest hematopoietic pro-

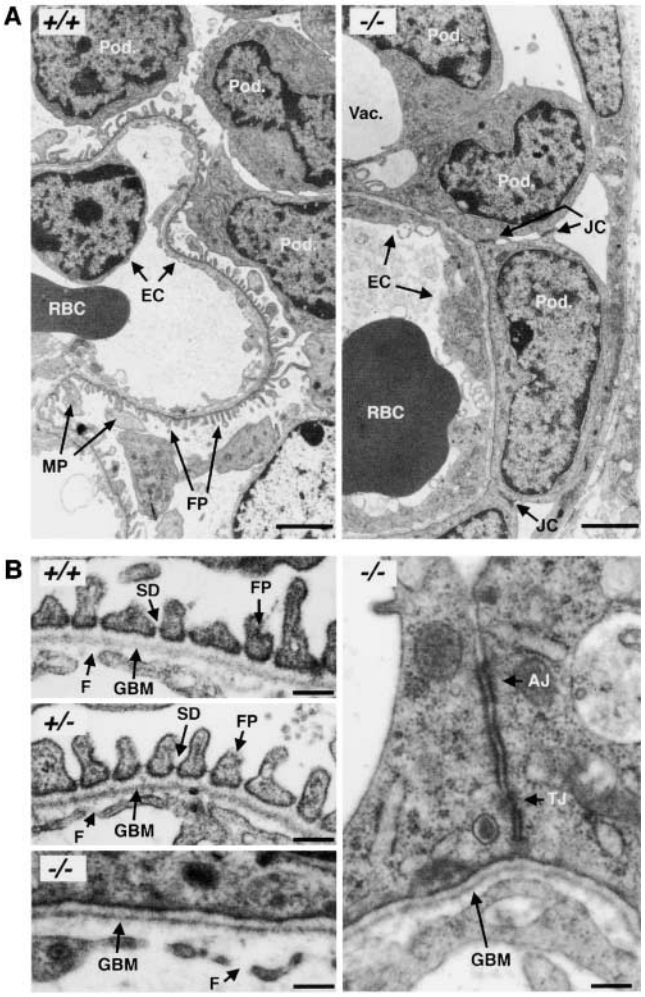

Figure 7. TEMs of embryonic day 18 kidneys from *podxl*$^{+/+}$ and *podxl*$^{-/-}$ embryos. (A) *podxl*$^{+/+}$ kidneys have normal podocytes (Pod.) with typical MPs and FPs that embrace the outer aspect of the capillary basement membrane. RBCs can be seen in the lumen of the endothelial vessels. *podxl*$^{-/-}$ show a complete loss of SDs and FPs. JCs are present between all of the *podxl*$^{-/-}$ podocytes. Podocytes in *podxl*$^{-/-}$ mice also display numerous vacuoles (Vac.) and overall the glomerular capillaries had a thicker EC layer (EC). Scale bars, 2 μm. (B) Higher magnification reveals that the SDs and FPs indicated by arrows in the *podxl*$^{+/+}$ and *podxl*$^{+/-}$ mice are completely lost in *podxl*$^{-/-}$ glomeruli. JCs including TJs and AJs are present between *podxl*$^{-/-}$ podocytes. The endothelial fenestrae (F) within the ECs can be found in wild-type controls but the fenestrae reduced in the *podxl*$^{-/-}$ glomerular capillaries. Scale bars, 0.2 μm.

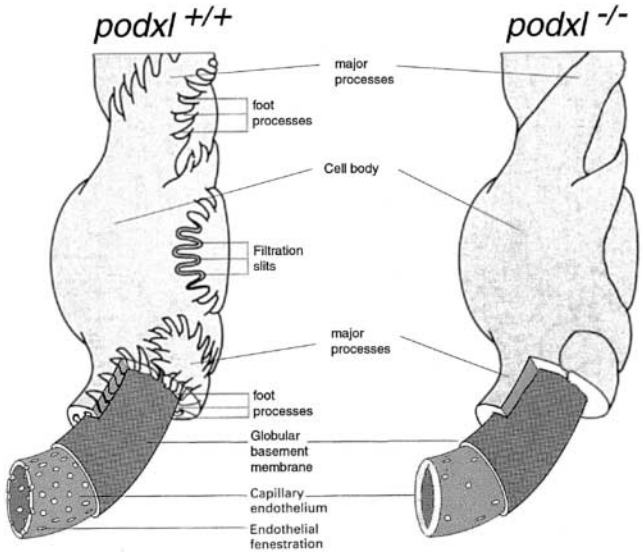

Figure 8. Schematic representation of the glomerular filter in wild-type and podocalyxin-deficient mice (adapted from reference 14). For ease of presentation, the mesangial cells that would normally link the capillary loops (disrupting the layer of podocytes) have been left out of the diagram. The lack of interdigitating FPs in the *podxl*$^{-/-}$ mice leads to a lack of filtration slit area. This, along with the decrease in the fenestration of the glomerular capillaries, is thought to lead to a decrease in the potential area for filtration and the anuria that occurs in the *podxl*$^{-/-}$ mice.

genitors, we performed an extensive analysis of the hematopoietic development in wild-type and podocalyxin-deficient mice. Hematopoietic tissues from *podxl*$^{+/+}$, *podxl*$^{+/-}$, and *podxl*$^{-/-}$ embryos were stained with antibodies to CD34, Sca-1, c-kit, Ter119, CD41, Mac1, Gr-1, B220, CD3, CD4, and CD8 to assess the numbers of hematopoietic progenitors and erythroid, megakaryocytic/platelet, myeloid, granulocytic, and B and T lineage cells, respectively. We observed no differences in the frequency or phenotype of any hematopoietic lineages in 15-d fetal liver, 18-d bone marrow, or 18-d spleen of *podxl*$^{-/-}$ embryos. Likewise, we observed no defects in the formation or localization of hematopoietic and vascular cells in podocalyxin-deficient yolk sac, lung, heart, liver, or gut. Thus, the data suggest that podocalyxin is either dispensable for the formation of these cell types, or its loss can be compensated for by other related molecules.

Discussion

In this study, we have generated mice lacking the sialomucin, podocalyxin. These mice die during the first day of life with severe kidney abnormalities and a pathology consistent with neonatal anuric renal failure. While some of the null mice had edema and/or displayed omphalocele, most appear normal at birth. Thus, despite the expression of podocalyxin by most vascular endothelia, a subset of mesothelial cells and hematopoietic stem cells, the abnormalities in the *podxl*$^{-/-}$ mice were largely confined to the kidney.

Role of Podocalyxin in Glomerular Structure and Function. In kidneys, the final stage of glomerular filtrate production occurs when the ultrafiltrate passes through the filtration slits between neighboring podocyte FPs. The specialized cell–cell junctions between podocyte FPs forming the slit diaphragm provides the last barrier for filtrate production (Fig. 8). The permeability of the glomerular filter is highly dependent on the filtration slit surface area and the filtration properties of the slit diaphragm (60, 61). The podocytes of *podxl*$^{-/-}$ mice do not form FPs or SDs and instead form impermeable TJs. The absence of SDs and the reduction of filtration slit area due to the lack of interdigitating FPs in the *podxl*$^{-/-}$ mice probably leads to

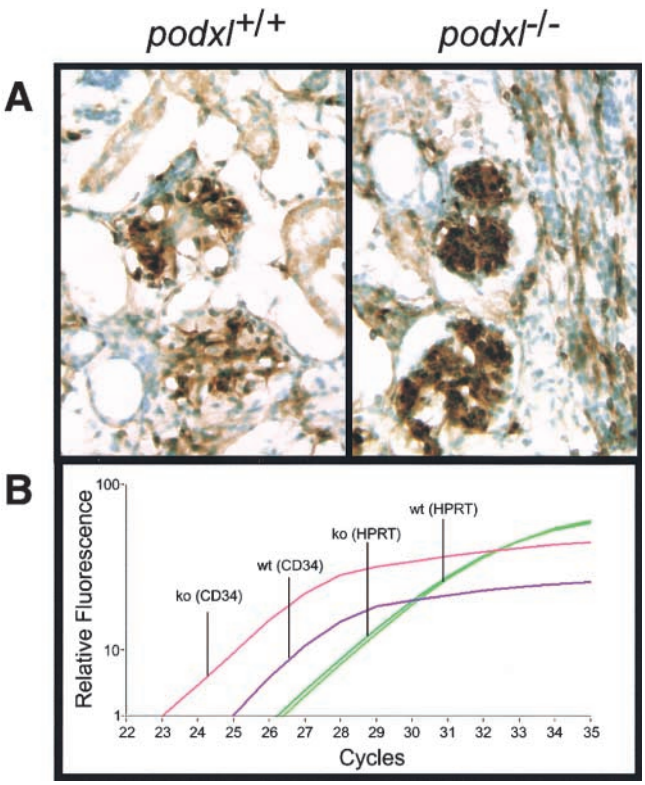

Figure 9. CD34 mRNA overexpression in kidney of *podxl*$^{-/-}$ 18-d embryos. (A) CD34 immunostaining of 18-d embryo kidneys. Brown stain represents CD34 antigen detected by immunoperoxidase stain; green stain represents methyl green counterstain of nuclei. (B) Relative quantification of CD34 and HPRT mRNA in 18-d embryo kidney by Real-Time reverse transcription PCR (LightCycler™; Roche). Y-axis, relative level of cDNA product as determined by SYBR Green™ fluorescence; X-axis, number of PCR cycles; Pink lines, *podxl*$^{-/-}$ mRNA with CD34 primers; purple lines, *podxl*$^{+/+}$ mRNA with CD34 primers; light green lines, *podxl*$^{-/-}$ mRNA with HPRT primers; dark green lines, *podxl*$^{+/+}$ mRNA with HPRT primers. One of four representative experiments with kidney mRNA from two independent mice of each genotype.

glomerular filters with reduced permeability that result in anuria at birth.

It has been speculated that the charge of podocalyxin is required for maintaining the spacing between FPs (15) since podocalyxin is the major constituent of the glycocalyx at their apical surface. This is supported by the fact that the inducible, ectopic expression of podocalyxin in Chinese hamster ovary cells and Madin-Darby canine kidney epithelial cells results in the inhibition of cell aggregation and in an altered organization of junctional proteins in adherent cell monolayers (62). Moreover, ectopic expression was shown to inhibit the formation of electrical-resistant monolayers of epithelial cells, indicating that podocalyxin can block the formation of TJs. Our data clearly support and extend this finding; in the absence of podocalyxin, JCs persist between podocytes and they fail to migrate down the lateral surface towards the basement membrane where they are normally modified to form SDs. The failure of the podocytes in *podxl*$^{-/-}$ mice to form permeable cell–cell junctions (SDs) is consistent with a role for podocalyxin as an antiadhesin on the surface of the podocytes and as a potential regulator of cell junctions.

It has been suggested that one way podocalyxin regulates cell–cell junctions is by interacting with the actin cytoskeleton, possibly via the actin-associated protein ezrin. The COOH-terminal tail of podocalyxin (D-T-H-L) is highly homologous to that of endoglycan and CD34 (D-T-H/E-L; Fig. 1 A). All three molecules contain the consensus sequence (X-S/T-X-V/I/L) recognized by proteins with PDZ protein interaction domains (63). PDZ-containing proteins can act as scaffolds to link transmembrane proteins in multiprotein complexes that may include the actin cytoskeleton (64). Indeed, one of us (unpublished data) recently found that the COOH terminus of podocalyxin interacts with NHERF-2, a PDZ domain-containing protein that can link transmembrane proteins to the actin cytoskeleton via ezrin (65). In light of the present studies we feel it is likely that this linkage is important in the modification of JCs in mature podocytes.

The vacuoles observed in the podocytes of *podxl*$^{-/-}$ mice are similar to the podocyte vacuoles seen in human or rodent models of renal disease (66–69). These vacuoles can occur in the setting of minimal change disease or in models where there is extensive podocyte injury (puromycin aminonucleoside–induced nephrosis). They have been hypothesized to result from the abnormal passage of fluid from the basolateral to apical surface of the podocyte in situations where there is extensive FP effacement or disruption of normal slit diaphrams (70, 71). Considering the lack of permeable cell–cell junctions and FPs in the *podxl*$^{-/-}$ mice, these podocyte vacuoles may result from the lack of a paracellular pathway for filtrate production and this "salvage pathway" may contribute to the bulk of fluid seen in the urinary space of the *podxl*$^{-/-}$ mice.

Podocalyxin Deficiency: Relation to other Podocyte-specific Mutations. Several proteins proposed to be involved in the formation of JCs between podocytes have been identified recently as crucial regulators of podocyte function. These include nephrin/NPHS1, podocin/NPHS2, CD2AP, P-cadherin, αβγ catenin, α-actinin-4, and ZO-1α (16, 20–23, 72). All of these proteins are expressed at the SDs between processes and have been speculated to participate in the formation of modified AJs (16, 26). Nephrin and P-cadherin are thought to interact by homotypic recognition and to be responsible for maintenance of the filtration slits (16, 20, 26). CD2AP has been shown to interact with the intracellular domain of nephrin (23) whereas αβγ catenins bind the intracellular domain of P-cadherin. Human mutations in NPHS2 or α actinin 4 result in proteinuria and FP effacement (21, 22). Ablation of CD2AP and nephrin in mice leads to nephrotic syndrome with massive proteinuria and effacement of the FPs. A striking difference between *podxl*$^{-/-}$ mice and mice lacking nephrin or CD2AP is that the latter mice exhibit massive proteinuria and are still able to develop podocyte FPs (20, 23) whereas the *podxl*$^{-/-}$ mice lack FPs and produce no urine. These results support the contention that podocalyxin has a fundamentally distinct function in podocyte cell

junctions (increased permeability) from nephrin/CD2AP (increased barrier function).

Aside from the proteins found in JCs, only a small number of other membrane proteins located at the apical surfaces of podocytes have been defined. They include podoplanin, a protein that is also expressed on nonpolarized cells (73), and GLEPP1, a transmembrane protein tyrosine phosphatase (38). GLEPP1 appears to regulate podocyte FP structure since deletion of this gene (ptpro) leads to toe-like podocyte FPs that are shorter and broader than the FPs of normal mice. Although *ptpro*$^{-/-}$ mice are viable and develop normally, they have a reduced glomerular filtration rate and after partial nephrectomy display a predisposition to hypertension. Thus, although the defects in *ptpro*$^{-/-}$ mice are much milder than those of *podxl*$^{-/-}$ mice, they also display a reduced glomerular filtration rate due to abnormalities in FP formation.

The fact that *podxl*$^{-/-}$ podocytes express the normal repertoire of both apical and junctional-complex podocyte markers suggests that maturation of these cells is relatively normal and that the observed defects in urine production are not due to defects in downstream protein expression. Rather, our results argue that podocalyxin loss leads directly to structural malformations of FPs. Similar to the neonatal lethality observed in *podxl*$^{-/-}$ mice, there are several other reports of anuric mice that die in the first day of life (52–55). However, it is noteworthy that most of these mutations result in much more severe kidney defects (agenesis) or in pleiotropic defects in other vital organs. Thus, podocalyxin loss represents the most selective, lethal anuria described to date.

Role of Podocalyxin in Resolution of Physiologic Omphalocele. In normal mouse development, the gut herniates into the umbilical space through the umbilical ring beginning at embryonic day 12 and retracts back into the peritoneal cavity by the 16th day of embryonic development (58). This "physiologic omphalocele" is resolved by the expansion of the peritoneal cavity and retraction of the gut from the umbilical cord. While only a subset of podocalyxin-null mice displayed omphalocele at birth, all null mice showed delay in omphalocele resolution in utero. Surprisingly, some heterozygotes showed a similar delay suggesting a dosage effect of this mucin on the resolution of omphalocele. Omphalocele is a relatively common congenital birth defect in man, affecting ~1:6,000 children, but the molecular details of its etiology are poorly understood. In many cases omphalocele has been linked to syndromes with abdominal organomegaly or defects in the development of the anterior abdominal wall leading to failure of umbilical ring closure (74). However, examination of *podxl*$^{-/-}$ mice revealed no abdominal organomegaly. Because of the dosage effect and because podocalyxin is expressed by the mesothelial cells lining the peritoneal membrane, we speculate that mesothelial function of this molecule is to provide an antiadhesive surface and facilitate retraction of the gut through the umbilical ring (see below).

Function and Redundancy of CD34-related Molecules in Development. Despite the widespread expression of sialomucins in many tissues their function is still poorly understood and, until now, ablation of sialomucins have not resulted in a lethal phenotype. This suggests that most sialomucins are either dispensable for normal development or that there are mechanisms that compensate for their loss such as redundancy. The *podxl*$^{-/-}$ mice provide the first example of a sialomucin that is critically required for the normal development and postnatal survival of mice. Since podocalyxin deficiency causes defects in tissues that selectively express podocalyxin but not CD34 (gut mesothelial cells and podocytes), while coexpressing tissues are spared (vascular endothelia and hematopoietic precursors), it is tempting to speculate that CD34 and podocalyxin can, indeed, cross-compensate. Our observation that CD34 expression is upregulated in *podxl*$^{-/-}$ mice is consistent with this idea and it will now be interesting to determine whether *podxl*$^{-/-}$/*cd34*$^{-/-}$ double KO mice exhibit hematopoietic and vascular defects (unpublished data).

Two opposing hypotheses have been proposed for the functions of the CD34 family of sialomucins: adhesion and antiadhesion. In favor of the adhesion model both podocalyxin and CD34, when expressed by HEVs, can act as adhesive tethers for activated leukocytes migrating into lymph nodes (8, 10). Lymphocytes use L-selectin (a C-type animal lectin) to bind to specific glycoforms of CD34 and podocalyxin expressed on the surface of HEVs and this is the initiating step in lymphocyte extravasation from blood into the lymph nodes. A caveat, however, is that L-selectin binding to these molecules is glycosylation specific and the appropriate modifications have usually only been observed on HEVs. Therefore, it is likely that in most tissues, podocalyxin and CD34 have alternate functions other than adhesion. Based on a number of studies, other researchers have speculated that podocalyxin (and in some circumstances CD34; reference 75) can act as an antiadhesion molecules or molecular "Teflon™" by virtue of its negatively charged mucin domain (1, 2, 15, 62, and see above).

One exciting hypothesis is that, in fact, these molecules can serve both adhesive and antiadhesive functions. Under the majority of circumstances, these molecules provide a barrier to adhesion, increase monolayer permeability, and aid in modifying JCs. In the special case of the HEVs, however, these molecules provide dual functions. In the first step they provide tethers for leukocytes expressing L-selectin binding. Subsequently, however, podocalyxin and CD34 move to the junctions between ECs where they act to "spread" the endothelia and facilitate leukocyte transmigration. This is consistent with previous reports showing movement of CD34 to junctions in response to cell activation (75). Analysis of mice lacking multiple members of the CD34 family offers an opportunity to test this model and should clarify this issue.

The authors wish to thank Dr. Pablo Labrador and Francesca Diella for assistance with construction of genetically modified mice, Monte Winslow and Mica DiCecco for assistance with genotyping

and PCR, and Meera Goyal and Lisa Riggs for assistance with tissue section analysis of kidneys. We also thank Drs. Jeffrey Miner for antibodies to laminin α5 and collagen α4(IV), Roger Wiggins for antibody to GLEPP1, Lawrence Holzman for antibody to mouse nephrin, Peter Mundel for antibody to synaptopodin, and Atsushi Miyajima and Takahiko Hara for antibody to mouse podocalyxin. Helpful suggestions and critical evaluation of this manuscript were provided by Drs. Peter Mundel, Jeffrey Miner, Hermann Ziltener, John Schrader, Ian Clark-Lewis, Fabio Rossi, Julie Nielsen, and Erin Drew. Special thanks to Maj Britt Hansen and MBH studies for advice, graphics, and prints.

C. Duhme was supported by the Boehringer Ingelheim Fonds. This work was funded by Canadian Medical Research Council grant MT-15477 (to K.M. McNagny) and National Institutes of Health grant DK02264-01A1 (to D.B. Kershaw) and an American Heart Association grant-in-aid (to D.B. Kershaw). K.M. McNagny is a Canadian Medical Research Council Scholar.

Submitted: 16 November 2000
Revised: 23 April 2001
Accepted: 15 May 2001

References

1. Kerjaschki, D., D.J. Sharkey, and M.G. Farquhar. 1984. Identification and characterization of podocalyxin-the major sialoprotein of the renal glomerular epithelial cell. *J. Cell Biol.* 98:1591–1596.
2. Dekan, G., C. Gabel, and M.G. Farquhar. 1991. Sulfate contributes to the negative charge of podocalyxin, the major sialoglycoprotein of the glomerular filtration slits. *Proc. Natl. Acad. Sci. USA.* 88:5398–5402.
3. Kershaw, D.B., P.E. Thomas, B.L. Wharram, M. Goyal, J.E. Wiggins, C.I. Whiteside, and R.C. Wiggins. 1995. Molecular cloning, expression and characterization of podocalyxin-like protein 1 from rabbit as a transmembrane protein of glomerular podocytes and vascular endothelium. *J. Biol. Chem.* 270:29439–29446.
4. Horvat, R., A. Hovorka, G. Dekan, H. Poczewski, and D. Kerjaschki. 1986. Endothelial cell membranes contain podocalyxin-the major sialoprotein of visceral glomerular epithelial cells. *J. Cell Biol.* 102:484–491.
5. McNagny, K.M., I. Pettersson, F. Rossi, I. Flamme, A. Shevchenko, M. Mann, and T. Graf. 1997. Thrombomucin, a novel cell surface protein that defines thrombocytes and multipotent hematopoietic progenitors. *J. Cell Biol.* 138: 1395–1407.
6. Miettinen, A., M.L. Solin, J. Reivinen, E. Juvonen, R. Vaisanen, and H. Holthofer. 1999. Podocalyxin in rat platelets and megakaryocytes. *Am. J. Pathol.* 154:813–822.
7. Hara, T., Y. Nakano, M. Tanaka, K. Tamura, T. Sekiguchi, K. Minehata, N.G. Copeland, N.A. Jenkins, M. Okabe, H. Kogo, et al. 1999. Identification of podocalyxin-like protein 1 as a novel cell surface marker for hemangioblasts in the murine aorta-gonad-mesonephros region. *Immunity.* 11:567–578.
8. Sassetti, C., K. Tangemann, M.S. Singer, D.B. Kershaw, and S.D. Rosen. 1998. Identification of podocalyxin-like protein as a high endothelial venule ligand for L-selectin: parallels to CD34. *J. Exp. Med.* 187:1965–1975.
9. Krause, D.S., M.J. Fackler, C.I. Civin, and W.S. May. 1996. CD34: structure, biology, and clinical utility. *Blood.* 87:1–13.
10. Baumhueter, S., M. Singer, W. Henzel, S. Hemmerich, M. Renz, S. Rosen, and L.A. Lasky. 1993. Binding of L-selectin to the vascular sialomucin CD34. *Science.* 262:436–438.
11. Cheng, J., S. Baumhueter, G. Cacalano, K. Carver-Moore, H. Thibodeaux, R. Thomas, H.E. Broxmeyer, S. Cooper, N. Hague, M. Moore, and L.A. Lasky. 1996. Hematopoietic defects in mice lacking the sialomucin CD34. *Blood.* 87:479–490.
12. Suzuki, A., D.P. Andrew, J.A. Gonzalo, M. Fukumoto, J. Spellberg, M. Hashiyama, H. Takimoto, N. Gerwin, I. Webb, G. Molineux, et al. 1996. CD34-deficient mice have reduced eosinophil accumulation after allergen exposure and show a novel crossreactive 90-kD protein. *Blood.* 87:3550–3562.
13. Sassetti, C., A. Van Zante, and S.D. Rosen. 2000. Identification of endoglycan, a member of the CD34/podocalyxin family of sialomucins. *J. Biol. Chem.* 275:9001–9010.
14. Burkitt, H.G., B. Young, and J.W. Heath. 1996. Wheater's Functional Histology. 3rd edition. J. Kilgore, editor. Churchill Livingston, New York. 282 pp.
15. Schnabel, E., G. Dekan, A. Miettinen, and G. Farquhar. 1989. Biogensis of podocalyxin. The major glomerular sialoglycoprotein in the new born rat kidney. *Eur. J. Cell. Biol.* 48:313–326.
16. Reiser, J., W. Kriz, M. Kretzler, and P. Mundel. 2000. The glomerular slit diaphragm is a modified adherens junction. *J. Am. Soc. Nephrol.* 11:1–8.
17. Seiler, M.W., M.A. Venkatachalam, and R.S. Cotran. 1975. Glomerular epithelium: structural alterations induced by polycations. *Science.* 189:390–393.
18. Seiler, M.W., H.G. Rennke, M.A. Venkatachalam, and R.S. Cotran. 1977. Pathogenesis of polycation-induced alteration ("fusion") of glomerular epithelium. *Lab. Invest.* 36:48–61.
19. Andrews, P.M. 1979. Glomerular epithelial alterations resulting from sialic acid surface coat removal. *Kidney Int.* 15:376–385.
20. Kestila, M., U. Lenkkeri, M. Mannikko, J. Lamerdin, P. McCready, H. Putaala, V. Ruotsalainen, T. Morita, M. Nissinen, R. Herva, et al. 1998. Positionally cloned gene for a novel glomerular protein, nephrin, is mutated in congenital nephrotic syndrome. *Mol. Cell.* 1:575–582.
21. Boute, N., O. Gribouval, S. Roselli, F. Benessy, H. Lee, A. Fuchshuber, K. Dahan, M.C. Gubler, P. Niaudet, and C. Antignac. 2000. NPHS2, encoding the glomerular protein podocin, is mutated in autosomal recessive steroid-resistant nephrotic syndrome. *Nat. Genet.* 24:349–354.
22. Kaplan, J.M., S.H. Kim, K.N. North, H. Rennke, L.A. Correia, H.Q. Tong, B.J. Mathis, J.C. Rodriguez-Perez, P.G. Allen, A.H. Beggs, and M.R. Pollak. 2000. Mutations in ACTN4, encoding alpha-actinin-4, cause familial focal segmental glomerulosclerosis. *Nat. Genet.* 24:251–256.
23. Shih, N.Y., J. Li, V. Karpitskii, A. Nguyen, M.L. Dustin, O. Kanagawa, J.H. Miner, and A.S. Shaw. 1999. Congenital nephrotic syndrome in mice lacking CD2-associated protein. *Science.* 286:312–315.
24. Kreidberg, J.A., M.J. Donovan, S.L. Goldstein, H. Rennke, K. Shepherd, R.C. Jones, and R. Jaenisch. 1996. α3β1 integrin has a crucial role in kidney and lung organogenesis. *Development.* 122:3537–3547.
25. Smoyer, W.E., and P. Mundel. 1998. Regulation of podocyte structure during the development of nephrotic syndrome. *J. Mol. Med.* 76:172–183
26. Somlo, S., and P. Mundel. 2000. Getting a foothold in nephrotic syndrome. *Nat. Genet.* 24:333–335.

27. Putaala, H., R. Soininen, P. Kilpelainen, J. Wartiovaara, and K. Tryggvason. 2001. The murine nephrin gene is specifically expressed in kidney, brain and pancreas: inactivation of the gene leads to massive proteinuria and neonatal death. *Hum. Mol. Genet.* 10:1–8.
28. Tybulewicz, V.L., C.E. Crawford, P.K. Jackson, R.T. Bronson, and R.C. Mulligan. 1991. Neonatal lethality and lymphopenia in mice with a homozygous disruption of the c-abl proto-oncogene. *Cell.* 65:1153–1163.
29. Sedlvy, J.M., and A.L. Joyner. 1993. Gene Targeting: A Practical Approach. Oxford University Press, Oxford. 208 pp.
30. Torres, D.M., and R. Kuhn. 1997. Laboratory protocols for conditional gene targeting. Oxford University Press, Oxford. 167 pp.
31. Feinberg, A.P., and B. Vogelstein. 1983. A technique for radiolabeling DNA restriction endonuclease fragments to high specific activity. *An. Biochem.* 132:6–13.
32. Sambrook, J., E.F. Fritsch, and T. Maniatus. 1989. Molecular Cloning: A Laboratory Manual. Cold Spring Harbor Laboratory, Cold Spring Harbor, NY. 147 pp.
33. Church, G.M., and W. Gilbert. 1985. The genomic sequencing technique. *Prog. Clin. Biol. Res.* 177:17–21.
34. Chomczynski, P., and N. Sacchi. 1987. Single-step method of RNA isolation by acid guanidinium thiocynate-phenol-chloroform extraction. *An. Biochem.* 162:156–159.
35. Dugaiczyk, A. 1983. Cloning and sequencing of a deoxyribonucleic acid copy of glyceraldehyde-3-phosphate dehydrogenase messenger ribonucleic acid isolated from chicken muscle. *Biochemistry.* 22:1605–1613.
36. Sharif, K., M. Goyal, D. Kershaw, R. Kunkel, and R. Wiggins. 1998. Podocyte phenotypes as defined by expression and distribution of GLEPP1 in the developing glomerulus and in nephrotic glomeruli from MCD, CNF, and FSGS. A dedifferentiation hypothesis for the nephrotic syndrome. *Exp. Nephrol.* 6:234–244.
37. Miner, J.H., and J.R. Sanes. 1994. Collagen IV α3, α4, and α5 chains in rodent basal laminae: sequence, distribution, association with laminins, and developmental switches. *J. Cell Biol.* 127:879–891.
38. Wharram, B.L., M. Goyal, P.J. Gillespie, J.E. Wiggins, D.B. Kershaw, L.B. Holzman, R.C. Dysko, T.L. Saunders, L.C. Samuelson, and R.C. Wiggins. 2000. Altered podocyte structure in GLEPP1 (Ptpro)-deficient mice associated with hypertension and low glomerular filtration rate. *J. Clin. Invest.* 106:1281–1290.
39. Unkeless, J.C. 1979. Characterization of a monoclonal antibody directed against mouse macrophage and lymphocyte Fc receptors. *J. Exp. Med.* 150:580–596.
40. Osawa, M., K. Hanada, H. Hamada, and H. Nakauchi. 1996. Long-term lymphohematopoietic reconstitution by a single $CD34^-$ low/negative hematopoietic stem cell. *Science.* 273: 242–245.
41. Aihara, Y., H.J. Buhring, M. Aihara, and J. Klein. 1986. An attempt to produce "pre-T" cell hybridomas and to identify their antigens. *Eur. J. Immunol.* 16:1391–1399.
42. Ikuta, K., and I.L. Weissman. 1992. Evidence that hematopoietic stem cells express mouse c-kit but do not depend on steel factor for their generation. *Proc. Natl. Acad. Sci. USA.* 89:1502–1506.
43. Springer, T., G. Galfre, D.S. Secher, and C. Milstein. 1978. Monoclonal xenogeneic antibodies to murine cell surface antigens: identification of novel leukocyte differentiation antigens. *Eur. J. Immunol.* 8:539–551.
44. Coffman, R.L. 1982. Surface antigen expression and immunoglobulin gene rearrangement during mouse pre-B cell development. *Immunol. Rev.* 69:5–23.
45. Leo, O., M. Foo, D.H. Sachs, L.E. Samelson, and J.A. Bluestone. 1987. Identification of a monoclonal antibody specific for a murine T3 polypeptide. *Proc. Natl. Acad. Sci. USA.* 84: 1374–1378.
46. Pierres, A., P. Naquet, A. Van Agthoven, F. Bekkhoucha, F. Denizot, Z. Mishal, A.M. Schmitt-Verhulst, and M. Pierres. 1984. A rat anti-mouse T4 monoclonal antibody (H129.19) inhibits the proliferation of Ia-reactive T cell clones and delineates two phenotypically distinct ($T4^+$, Lyt-2,3^-, and $T4^-$, Lyt-2,3^+) subsets among anti-Ia cytolytic T cell clones. *J. Immunol.* 132:2775–2782.
47. Ledbetter, J.A., and L.A. Herzenberg. 1979. Xenogeneic monoclonal antibodies to mouse lymphoid differentiation antigens. *Immunol. Rev.* 47:63–90.
48. Kina, T., K. Ikuta, E. Takayama, K. Wada, A.S. Majumdar, I.L. Weissman, and Y. Katsura. 2000. The monoclonal antibody TER-119 recognizes a molecule associated with glycophorin A and specifically marks the late stages of murine erythroid lineage. *Br. J. Haematol.* 109:280–287.
49. Fleming, T.J., M.L. Fleming, and T.R. Malek. 1993. Selective expression of Ly-6G on myeloid lineage cells in mouse bone marrow. RB6-8C5 mAb to granulocyte-differentiation antigen (Gr-1) detects members of the Ly-6 family. *J. Immunol.* 151:2399–2408.
50. Graf, T., K. McNagny, G. Brady, and J. Frampton. 1992. Chicken "erythroid" cells transformed by the gag-myb-ets-encoding E26 leukemia virus are multipotent. *Cell.* 70:201–213.
51. Kaufman, M.H. 1998. The Atlas of Mouse Development. Academic Press, Toronto. 525 pp.
52. Bullock, S.L., J.M. Fletcher, R.S. Beddington, and V.A. Wilson. 1998. Renal agenesis in mice homozygous for a gene trap mutation in the gene encoding heparan sulfate 2-sulfotransferase. *Genes Dev.* 12:1894–1906.
53. Davis, A.P., D.P. Witte, H.M. Hsieh-Li, S.S. Potter, and M.R. Capecchi. 1995. Absence of radius and ulna in mice lacking hoxa-11 and hoxd-11. *Nature.* 375:791–795.
54. Muller, U., D. Wang, S. Denda, J.J. Meneses, R.A. Pedersen, and L.F. Reichardt. 1997. Integrin α8β1 is critically important for epithelial-mesenchymal interactions during kidney morphogenesis. *Cell.* 88:603–613.
55. Pellegrini, M., A. Mansouri, A. Simeone, E. Boncinelli, and P. Gruss. 1996. Dentate gyrus formation requires Emx2. *Development.* 122:3893–3898.
56. Thomas, P.E., B.L. Wharram, M. Goyal, J.E. Wiggins, L.B. Holzman, and R.C. Wiggins. 1994. GLEPP1, a renal glomerular epithelial cell (podocyte) membrane protein tyrosine phosphatase. Identification, molecular cloning, and characterization in rabbit. *J. Biol. Chem.* 269:19953–19962.
57. Wang, R., P.L. St. John, M. Kretzler, R.C. Wiggins, and D.R. Abrahamson. 2000. Molecular cloning, expression, and distribution of glomerular epithelial protein 1 in developing mouse kidney. *Kidney Int.* 57:1847–1859.
58. Mundlos, S., J. Pelletier, A. Darveau, M. Bachmann, A. Winterpacht, and B. Zabel. 1993. Nuclear localization of the protein encoded by the Wilms' tumor gene WT1 in embryonic and adult tissues. *Development.* 119:1329–1341.
59. Mundel, P., H.W. Heid, T.M. Mundel, M. Kruger, J. Reiser, and W. Kriz. 1997. Synaptopodin: an actin-associated

protein in telencephalic dendrites and renal podocytes. *J. Cell Biol.* 139:193–204.
60. Drumond, M.C., and W.M. Deen. 1994. Structural determinants of glomerular hydraulic permeability. *Am. J. Physiol.* 266:F1–F12.
61. Kriz, W., M. Kretzler, A.P. Provoost, and I. Shirato. 1996. Stability and leakiness: opposing challenges to the glomerulus. *Kidney Int.* 49:1570–1574.
62. Takeda, T., W.Y. Go, R.A. Orlando, and M.G. Farquhar. 2000. Expression of podocalyxin inhibits cell-cell adhesion and modifies junctional properties in madin-darby canine kidney cells. *Mol. Biol. Cell.* 11:3219–3232.
63. Songyang, Z., A.S. Fanning, C. Fu, J. Xu, S.M. Marfatia, A.H. Chishti, A. Crompton, A.C. Chan, J.M. Anderson, and L.C. Cantley. 1997. Recognition of unique carboxyl-terminal motifs by distinct PDZ domains. *Science.* 275:73–77.
64. Fanning, A.S., and J.M. Anderson. 1999. Protein modules as organizers of membrane structure. *Curr. Opin. Cell Biol.* 11: 432–439.
65. Shenolikar, S., and E.J. Weinman. 2001. NHERF: targeting and trafficking membrane proteins. *Am. J. Physiol. Renal Physiol.* 280:F389–F395.
66. Toth, T., and S. Takebayashi. 1992. Glomerular podocyte vacuolation in idiopathic membranous glomerulonephritis. *Nephron.* 61:16–20.
67. Yoshikawa, N., H. Ito, R. Akamatsu, H. Hazikano, S. Okada, and T. Matsuo. 1986. Glomerular podocyte vacuolation in focal segmental glomerulosclerosis. *Arch. Pathol. Lab. Med.* 110:394–398.
68. Andrews, P.M. 1977. A scanning and transmission electron microscopic comparison of puromycin aminonucleoside-induced nephrosis to hyperalbuminemia-induced proteinuria with emphasis on kidney podocyte pedicel loss. *Lab. Invest.* 36:183–197.
69. Caulfield, J.P., J.J. Reid, and M.G. Farquhar. 1976. Alterations of the glomerular epithelium in acute aminonucleoside nephrosis. Evidence for formation of occluding junctions and epithelial cell detachment. *Lab. Invest.* 34:43–59.
70. Venkatachalam, M.A., M.J. Karnovsky, and R.S. Cotran. 1969. Glomerular permeability. Ultrastructural studies in experimental nephrosis using horseradish peroxidase as a tracer. *J. Exp. Med.* 130:381–399.
71. Venkatachalam, M.A., R.S. Cotran, and M.J. Karnovsky. 1970. An ultrastructural study of glomerular permeability in aminonucleoside nephrosis using catalase as a tracer protein. *J. Exp. Med.* 132:1168–1180.
72. Balda, M.S., and J.M. Anderson. 1993. Two classes of tight junctions are revealed by ZO-1 isoforms. *Am. J. Physiol.* 264: C918–C924.
73. Matsui, K., S. Breiteneder-Geleff, and D. Kerjaschki. 1998. Epitope-specific antibodies to the 43-kD glomerular membrane protein podoplanin cause proteinuria and rapid flattening of podocytes. *J. Am. Soc. Nephrol.* 9:2013–2026.
74. Kilby, M.D., A. Lander, and M. Usher-Somers. 1998. Exomphalos (omphalocele). *Prenat. Diagn.* 18:1283–1288.
75. Delia, D., M.G. Lampugnani, M. Resnati, E. Dejana, A. Aiello, E. Fontanella, D. Soligo, M.A. Pierotti, and M.F. Greaves. 1993. CD34 expression is regulated reciprocally with adhesion molecules in vascular endothelial cells in vitro. *Blood.* 81:1001–1008.